

Autoencoder Node Saliency: Selecting Relevant Latent Representations

Ya Ju Fan^a

^a*Center for Applied Scientific Computing, Lawrence Livermore National Laboratory,
Livermore, CA 94551, United States*

Abstract

The autoencoder is an artificial neural network model that learns hidden representations of unlabeled data. With a linear transfer function it is similar to the principal component analysis (PCA). While both methods use weight vectors for linear transformations, the autoencoder does not come with any indication similar to the eigenvalues in PCA that are paired with the eigenvectors. We propose a novel supervised node saliency (SNS) method that ranks the hidden nodes by comparing class distributions of latent representations against a fixed reference distribution. The latent representations of a hidden node can be described using a one-dimensional histogram. We apply normalized entropy difference (NED) to measure the “interestingness” of the histograms, and conclude a property for NED values to identify a good classifying node. By applying our methods to real data sets, we demonstrate the ability of SNS to explain what the trained autoencoders have learned.

Keywords: Autoencoder, latent representations, unsupervised learning, neural networks, node selection

1. Background and Motivation

Autoencoders aim to find an encoding for a data set in a reduced dimension [1]. It is done by operating the encoding and decoding of the data, arranged in series, while minimizing the reconstruction error. The encoding of autoencoders constructs a powerful representation and often learns useful properties of the data [2]. It is unsupervised because class labels (i.e. responses of the observations) used for classifying the data points (or observations) are not considered when building autoencoders.

An autoencoder is designed in a way that input data are not perfectly reconstructed, forcing the algorithm to learn meaningful properties of the data. This is, in particular, useful when data labels are highly unbalanced or contain human faults. One example is in biomedical research. Records have been shown

Email address: fan4@llnl.gov (Ya Ju Fan)

that a massive proportion of cell lines is mislabeled [3, 4], causing potentially erroneous findings. In addition, the majority of cell line samples tends to have positive responses, producing unbalanced data.

Supervised learning methods use labels to guide the training algorithm whose performance is sensitive to the quality of the labels. A frequent problem is that when a method tries to minimize an average classification accuracy, it tends to label all data points to the major class and sacrifice the accuracy of the minority. Unsupervised learning methods do not consider any information about the labeled responses, and hence have no sensitivity to the labels.

An autoencoder with linear transfer functions is similar to the well known principal component analysis (PCA). Given a data matrix $\mathbf{X} \in \mathbb{R}^{n \times d}$ that consists of n data points of d dimensions in real numbers, PCA takes the d -dimensional data and finds a smaller number (denoted by m where $m < d$) of orthogonal directions where the data have the most variance. Using the singular value decomposition on the data matrix, we generate the eigenvectors corresponding to the largest eigenvalues. These eigenvectors are called the principal components, which are the orthogonal directions to project the data into a lower dimensional space. The advantage of PCA is that each of the corresponding eigenvalues is related to the variance in the data at each of the directions. The direction of the first principal component is the direction of the greatest variance in the data, and the directions of the succeeding principal components are orthogonal to the preceding components while having the highest variance possible. Therefore, we can sort the eigenvalues and know how many of the top m eigenvectors need to keep to ensure a sufficient amount of variance in a lower dimensional representation.

The autoencoder algorithm transforms a data set using a weight matrix and an activation function. The encoded data can be approximately reconstructed using the same weight matrix and activation function. The aim of the algorithm is to find the optimal weight matrix with the least possible amount of distortion. For a total number of m hidden nodes, the weight matrix contains m weight vectors of dimension d , each for a hidden node.

If we use m hidden nodes in an autoencoder with a linear transfer function and minimize the squared reconstruction error for the same data set, the optimal m weight vectors will span the space as the first m components found by PCA [5]. The difference in autoencoder is that the weight vectors from the hidden nodes may not be orthogonal, and they are not designed to be the directions of the largest variances [1]. Especially there exist no indications that are equivalent to the eigenvalues of PCA that can evaluate the weight vectors in an autoencoder according to their relevance to the data.

Motivated by the limitation of lacking the indications, this paper proposes novel node saliency methods that can be used to rank the hidden nodes based on their relevance to a given learning task. Our objective is to explain what the trained autoencoders have learned when being unsupervised. In this paper, we will show that our node saliency methods provide three useful insights:

1. To evaluate how a hidden node performs a selected learning task.

2. To identify redundant hidden nodes that can be trimmed down for a more concise network structure.
3. To reveal explanatory input features from the identified node that gives high learning performance.

In most neural networks, the number of hidden nodes in a hidden layer is user-defined and without a clear guide. We know that a hidden node is redundant if its latent representations are nearly constant. Conversely, if no redundant nodes exist, we may need to increase the number of hidden nodes for a model to excel. High performance nodes provide weights on features from the previous layer, and hence to explain a learning process becomes possible after they are identified.

The rest of the paper is organized as follows. Section 2 reviews related works. Section 3 reviews the autoencoder algorithm. Section 4 proposes the node saliency approaches, followed by the experimental settings in Section 5, including the description of real data sets and the training of autoencoders. In Section 6 we discuss the empirical results of the node saliency methods. Finally, Section 7 concludes the study.

2. Related work

Autoencoders have been applied on genome-wide assays of cancer for knowledge extraction using their unsupervised nature [6, 7]. A denoising autoencoder is trained on the breast cancer gene expression data, where a hidden node that best classifies the data is obtained through cross validation on multiple activation thresholds [6]. More insights are obtained that could link specific features to biological pathways. In [7], variational autoencoders are built on the Cancer Genome Atlas (TCGA) data sets of genomic features profiled over various cancer types. A quick search for explanatory features are obtained by subtracting a series of mean values of latent representations.

To interpret the learning behavior of neural networks, methods in [8] make perturbations to individual inputs and observe the impact on later nodes in the network. DeepLIFT [9] learns important features in neural networks through propagating activation differences that compare the activation of each node to its reference activation and assign contribution scores according to the difference. A saliency map of input images is computed in [10] for visualization of image classification in deep convolutional networks. These methods are focused on behaviors of input data in the paths of networks.

Gilles [11] defined saliency based on local signal complexity for matching and register two images. The method computes Shannon entropy of local attributes in a neighborhood around the current pixel. Image area with higher signal complexity has a flatter distribution of pixel intensities and thus a higher entropy; while a plain image region has one peaked distribution and a lower entropy. Scale saliency [12] includes a measure of the statistical dissimilarity across scale to the saliency method, which is applied in [13] for tracking moving objects in videos.

The analysis of histograms on signals has been applied for finding useful (interesting) relationships that look far from random, describing the state of the system and then, possibly, detecting faulty operation. The consensus self-organizing models (COSMO) approach [14] has been used for detecting faults on vehicle fleets. A method for comparing signals based on histograms in [15] displays a success in handling deviations in real data. Analyses of signal “interestingness” using histograms appear in [16] aiming at autonomous knowledge discovery to build fault detection. These approaches are used in engineering problems and not yet applied to analyze neural networks.

One can also compute pairwise comparison of histograms. A review on measures for quantifying the difference between two histograms can be found in [17]. [18] presents an overview of histogram distance measures. The pairwise comparison is useful for detecting deviating signals. We are not interested in comparing two histograms at a time due to its cumbersome pairwise results and the wide selection of distance measures.

To summarize, our proposed node saliency methods are focused on comparing histograms of latent representations by ranking hidden nodes. The evaluation is based on a comparison between the distribution of class labels and a fixed reference distribution. We propose a novel supervised node saliency (SNS) method for ranking hidden nodes. Another novelty of our contribution is that we link two methods from other engineering applications to understand the distribution of latent representations, including the normalized entropy difference (NED) and the use of histograms in scale saliency.

3. Autoencoder review

In this section, we review the autoencoder algorithm and explain how the latent representations are generated.

3.1. Notation

Throughout the paper, matrices are denoted by bold uppercase letters, vectors by bold lowercase letters and scalars by letters not in bold. Let \mathbf{X} be a matrix whose i -th row vector is \mathbf{x}_i , and \mathbf{b} be a vector whose s -th element is b_s . The element at the i -th row and the j -th column of \mathbf{X} is $x_{i,j}$. We denote $\mathbf{1}$ as a vector of all ones with a suitable dimension. The cardinality of a set T is $|T|$.

3.2. Autoencoder

The simplest form of an autoencoder is a single layer, fully connected neural network with the output layer having the same number of nodes as the input layer [19]. The purpose of this architecture is to approximately reconstruct its own inputs. Usually the model restricts autoencoders in a way that allows them to not simply learn the input set perfectly. In this way autoencoders often learn useful properties of the data by forcing the model to prioritize which aspects of the input should be kept [2].

We denote a data set as $\mathbf{X} \in [0, 1]^{n \times d}$ that contains n data points $\mathbf{x}_i \in [0, 1]^d$ of d -dimensional variables for $i = 1, \dots, n$. To satisfy this definition, a data set that contains real numbers can be scaled to the range between zero and one, using the minimum and the maximum values at each dimension. The network of an autoencoder consists of two parts, the encoder function $\mathbf{A} = f(\mathbf{X}) \in [0, 1]^{m \times n}$ and the decoder $\mathbf{X}' = g(\mathbf{A}) \in [0, 1]^{n \times d}$. The encoder performs dimension reduction on the input and transforms the data of dimension d to a reduced dimension m where $m < d$. The decoder performs a reconstruction, mapping the data from the reduced dimension m back to the original dimension d . The objective function for this learning process is to minimize a loss function

$$L(\mathbf{X}, g(f(\mathbf{X}))),$$

where L is a loss function measuring the reconstruction error, the difference between the input data and the reconstructed data.

In a hidden layer where there are m hidden nodes, the encoder contains decision variables $\mathbf{W} \in \mathbb{R}^{m \times d}$ and $\mathbf{b} \in \mathbb{R}^m$ for an autoencoder to take the input \mathbf{X} and map it to the code \mathbf{A} using an activation function σ , where \mathbf{W} is a weight matrix and \mathbf{b} is a bias vector. A data point $\mathbf{x} \in [0, 1]^d$ is mapped to a vector of activation $\mathbf{a} \in [0, 1]^m$ where

$$\mathbf{a} = f(\mathbf{x}) = \sigma(\mathbf{W}\mathbf{x}^\top + \mathbf{b}).$$

The element a_s of \mathbf{a} is also called the *latent representation* of \mathbf{x} at node s for $s = 1, 2, \dots, m$. The decoder then maps the activation \mathbf{a} to the reconstruction \mathbf{x}' to the same dimensional space of \mathbf{x} where

$$\mathbf{x}' = g(\mathbf{a}) = \sigma(\mathbf{W}'\mathbf{a} + \mathbf{b}')^\top.$$

The weight matrix of the decoder \mathbf{W}' is often chosen as the transpose of the weight matrix in the encoder, that is $\mathbf{W}' = \mathbf{W}^\top$; and $\mathbf{b}' \in \mathbb{R}^d$ is the bias term in the decoder.

The autoencoder is trained by finding optimal solutions for \mathbf{W} , \mathbf{b} and \mathbf{b}' that minimize a loss function. We use the mean squared error (defined in (1)) and the cross-entropy loss (defined in (2)) to measure the difference between the input data \mathbf{x} and the reconstructed data \mathbf{x}' .

$$L_{MSE}(\mathbf{x}, \mathbf{x}') = \frac{1}{d} \sum_{j=1}^d (\mathbf{x}_j - \mathbf{x}'_j)^2. \quad (1)$$

$$L_{CE}(\mathbf{x}, \mathbf{x}') = - \sum_{j=1}^d [\mathbf{x}_j \cdot \log \mathbf{x}'_j + (1 - \mathbf{x}_j) \cdot \log(1 - \mathbf{x}'_j)]. \quad (2)$$

We use the sigmoid function for the activation function σ :

$$\sigma(z) = \frac{1}{1 + e^{-z}}, \quad (3)$$

which transforms the input values to the activation values that are mostly either close to zero or close to one. Restricting the algorithm from simply learning the data set $g(f(\mathbf{X})) = \mathbf{X}$, an autoencoder is driven to capture the most salient features of the input data.

4. Proposed node saliency methods

After training an optimal autoencoder for a data set, we are interested in exploring what has been learned in the autoencoder. Given a hidden node s (for $s = 1, \dots, m$), a set of data \mathbf{X} is transformed to its latent representations:

$$\mathbf{a}_s = \sigma(\mathbf{w}_s^* \mathbf{X}^\top + b_s^* \cdot \mathbf{1}), \quad (4)$$

which is also called the activation values at node s . The vector \mathbf{a}_s at node s can be described using a one-dimensional histogram. We assume that the activation values are in the range of $(0, 1)$, which can be obtained by selecting an activation function (i.e. sigmoid function) that restricts the range of projection. A histogram contains a set of k bin ranges, $B = \{[0, \frac{1}{k}), [\frac{1}{k}, \frac{2}{k}), \dots, [\frac{k-1}{k}, 1]\}$, where $[a, b)$ indicates values $\geq a$ and $< b$. Simply, the r -th bin range in the set B is $B_r = [\frac{r-1}{k}, \frac{r}{k})$ for $r = 1, \dots, k$. In this paper, we propose the node saliency methods that are based on the histograms of activation values. First, we define the unsupervised node saliency that measures the “interestingness” of histograms. Then, we propose a novel supervised node saliency that incorporates the distribution of class labels in the histograms and evaluates the classification ability of the hidden nodes.

4.1. Unsupervised node saliency

We begin with constructing a histogram of activation values for each hidden node s . Let n be the number of data points that are encoded to the latent representations. The entropy of the latent representations at a hidden node s is defined using the information in the histogram:

$$E(\mathbf{a}_s) = - \sum_r p(B_r, \mathbf{a}_s) \log_2 p(B_r, \mathbf{a}_s),$$

where $p(B_r, \mathbf{a}_s)$ is the probability of the activation values \mathbf{a}_s at node s occurring in the r -th bin range for $r = 1, \dots, k$ and $s = 1, \dots, m$. Precisely,

$$p(B_r, \mathbf{a}_s) \equiv \frac{|\{i \mid a_{s,i} \in B_r\}|}{|\mathbf{a}_s|}, \quad (5)$$

where $|\mathbf{a}_s| = n$. The entropy is dependent on how the bin sizes are adopted; it is proportional to the logarithm of the number of bins in the histogram. To compare two histograms with different numbers of values in the bins (i.e. two different latent variables), we use a normalized entropy difference (NED) [16]:

$$\begin{aligned} \text{NED}(\mathbf{a}_s) &= \frac{\log_2 \hat{k} - E(\mathbf{a}_s)}{\log_2 \hat{k}} \\ &= 1 + \frac{1}{\log_2 \hat{k}} \sum_r p(B_r, \mathbf{a}_s) \log_2 p(B_r, \mathbf{a}_s). \end{aligned} \quad (6)$$

Specifically we use \hat{k} , the number of occupied bins, instead of k , the number of bins in the histogram, to remove the effect of many empty bins. Note that $\log_2 \hat{k}$ is the maximum possible for $E(\mathbf{a}_s)$ when $p(B_r, \mathbf{a}_s) = 1/\hat{k}$ for all occupied bins. We define the *unsupervised node saliency* as the NED on the distribution of activation values at a hidden node, which can be used to rank the hidden nodes in order of their “interestingness”.

The normalized entropy difference satisfies $0 \leq \text{NED} \leq 1$. When NED equals one, it means a constant (or near constant activation values) that occupies (or occupy) only one bin. The hidden node that projects data to near constant values loses information and thus is less desirable to keep. A high value of NED indicates that most of the activation values are settled in few bins, so is a more “interesting” situation. Data represented in the nodes of high NED are organized into a few distinct groups that may highlight certain interesting characters. In contrast, a low value of NED suggests that the activation values are spread evenly over all the bins in the histogram, indicating an “uninteresting” case. Latent representations with low NED still contain information, but have less obvious clusters within them. Node saliency increases with NED, except for the extreme case when NED equals one.

The distribution of the activation values at a hidden node also depends on the choice of activation functions. Most activation functions in neural networks try to capture the rate of action potential, whose simplest form is a binary function. We use a sigmoid function (as shown in (3)) to handle such problems where the action frequency increases quickly at first, but gradually approaches an asymptote at 100 percent action. Because most values are restricted to be close to zero or close to one, data transformed to a node using a sigmoid function is less possible to have a low value of NED.

4.2. Properties for a good classifying node

In supervised learning, one of the tasks is to classify data points into two possible classes generically labeled 0 and 1. For each data point \mathbf{x}_i , there is a corresponding class label $y_i \in \{0, 1\}$ for $i = 1, \dots, n$. We apply the previously defined NED (in Section 4.1), and evaluate the class distribution of latent representations by computing NED separately for each class. The autoencoders are trained without including class labels. Thus, we are interested in examining whether the features constructed by autoencoders exhibit properties related to known class labels. We define $p_c(B_r, \mathbf{a}_s)$ as the probability of the values within the bin range B_r occurring in the activation that are of class c , that is

$$p_c(B_r, \mathbf{a}_s) \equiv \frac{|\{i \mid a_{s,i} \in B_r \text{ and } y_i = c\}|}{n_c},$$

where n_c is the number of data points in class c for $c = \{0, 1\}$. Using (6) for each of the classes, we obtain a supervised NED for class c defined as:

$$\text{NED}_c(\mathbf{a}_s) = 1 + \frac{1}{\log_2 \hat{k}} \sum_r p_c(B_r, \mathbf{a}_s) \log_2 p_c(B_r, \mathbf{a}_s). \quad (7)$$

If a node is a good classifier for two classes, it will tend to have most activation values from one class take up only the few bins in the histogram, which are different from the bins where the majority of the other class occupy. Since the activation values from both classes occupy the union of these bins, the data distribution combining both classes is less “interesting” than the data distribution of each single class. This leads to a condition that a good classifying node tends to have both $NED < NED_0$ and $NED < NED_1$ when NED is calculated using the union of both classes.

4.3. Supervised node saliency

In this section, we propose supervised node saliency (SNS) to evaluate the classification ability of hidden nodes. To make full use of the histograms, SNS employs a combined distribution of two given classes. The idea of SNS is derived from cross-entropy, whose function is to compare a distribution \mathbf{q} against a fixed reference distribution \mathbf{p} . When $\mathbf{p} = \mathbf{q}$, the cross-entropy is at its minimal value, which is the entropy of \mathbf{p} . In order to understand the differences among the nodes in their ability to separate two classes, we compare the combined distribution to a desired fixed reference distribution. We construct the distribution \mathbf{q} based on the activation values and their class distributions that vary at different hidden nodes. We manually design the fixed reference distribution \mathbf{p} using distributions of prospected data labels.

First, we are given two class labels (i.e. class 0 and class 1) that are of significant interests. We generate activation values for the hidden nodes using the optimal weight vector \mathbf{W}^* and the bias term \mathbf{b}^* on data points that belong to the two classes. For each node s in the hidden layer, a histogram is calculated for each of the two classes. We combine the two histograms and use the frequency of the two class labels as the class prediction produced by the hidden node s . Originally, we assume that an activation value being close to one indicates that it has high probability of coming from class 1. Without loss of generality, this assumption will be removed and addressed at the end of this section. Specifically in a histogram, we let q_r be the probability of being class 1 among all activation values that fall in bin range B_r , and define

$$\begin{aligned} q_r &= \text{prob}(y_i = 1 \mid a_{s,i} \in B_r) \\ &\equiv \frac{|\{i \mid a_{s,i} \in B_r \text{ and } y_i = 1\}|}{|\{i \mid a_{s,i} \in B_r\}|}. \end{aligned} \quad (8)$$

This definition implies that $1 - q_r = \text{prob}(y_i = 0 \mid a_{s,i} \in B_r)$ is the probability of being class 0 among all activation values that fall in bin range B_r .

Next, we design two distributions for the fixed reference distribution $\mathbf{p} = [p_1, \dots, p_k]$. In order to compare with the class distribution $\mathbf{q} = [q_1, \dots, q_k]$, we define the fixed reference distributions in a form of histograms with the same number of bins, bin widths and value ranges. Let p_r be the reference probability of being class 1 in bin r for $r = 1, \dots, k$ in the histogram. The two reference probability distributions are defined in the following equations:

- Increasing probability distribution:

$$p_r = \frac{2r-1}{2k} \quad \text{for } r = 1, \dots, k. \quad (9)$$

- Binary distribution:

$$p_r = \begin{cases} 0 & \text{if } r < k/2 \\ 1 & \text{if } r \geq k/2. \end{cases} \quad (10)$$

A good classifying node is expected to have a class distribution similar to the fixed reference distribution. The first layout of the fixed reference distribution is arranged as an increasing probability distribution defined in (9). In this formulation, the middle values (mid-point values) in the value range of each bin are used to form the histogram \mathbf{p} . In practice, this setting is attainable due to the restricted activation values made by the sigmoid function that are bounded between zero and one. For a histogram with $k = 10$ bins that are of equal width, we have $\mathbf{p} = [0.05, 0.15, \dots, 0.95]$. The class *prediction* q_r defined in (8) is the probability of the activation values that fall in each bin r and of class 1. Using the increasing probability distribution as a fixed reference distribution, we expect that the probability q_r of a latent representation being class 1 increases as the bin range r moves toward its maximum.

The second design of the fixed reference is a binary distribution as defined in (10). In this setting, we prefer that all activation values from one class gather in half of the bin intervals, while values from the other class gather in the other half of the bins. In other words, an optimal hidden node is able to form two clusters that are clearly distinguishable. Therefore, we have the reference probability p_r at bin r equal to 100% for the half of the bins where activation values are close to one, and equal to zero for the rest of the bins. By comparing the class distribution with this binary distribution, we evaluate the classification performance of the hidden nodes.

Depending on the distribution of activation values, the number of data points fall in a bin may vary greatly among different bins, especially in the “interesting” nodes where the activation values are settled in a few bins. Therefore, if we use a weight on the cross-entropy of each bin r , i.e. $p(B_r, \mathbf{a}_s)$ as in (5), then we are able to emphasize the class distribution of the bin that contains most data points, soften the effect of the bin where very few points exist, and ignore all the empty bins. As a result, only the occupied bins will be considered, so the effect of many unused bins is removed, and undefined logarithms are also avoided.

So far, we have assumed that an activation value close to one indicates a higher probability that the data point is from class 1, and a value close to zero is more likely from class 0. With this assumption, we define the weighted cross entropy for class 1 (WCE_1) as follows:

$$\text{WCE}_1 \equiv \sum_r p(B_r, \mathbf{a}_s) \left[-p_r \log_2 q_r - (1 - p_r) \log_2 (1 - q_r) \right]. \quad (11)$$

Since the activation values are generated from training an autoencoder without using any class labels, there exists no reference on which of the two classes that the activation value equals to one refers to. In practice, a high activation value can possibly come from class 0 as well. Thus, we measure the two possible values for each class. If the probability of an activation value being class 1 is p , then the probability of being class 0 is $1 - p$. We define the weighted cross entropy for class 0 (WCE_0) as follows:

$$\text{WCE}_0 \equiv \sum_r p(B_r, \mathbf{a}_s) \left[- (1 - p_r) \log_2 q_r - p_r \log_2 (1 - q_r) \right], \quad (12)$$

by swapping the class labels 1 and 0. Finally, the supervised node saliency (SNS) for a node s takes the smaller value of WCE_0 and WCE_1 , which is defined as:

$$\text{SNS} \equiv \min \{ \text{WCE}_0, \text{WCE}_1 \}. \quad (13)$$

Our SNS evaluates how the class distribution in latent representations is different from the fixed reference distribution. A smaller value of SNS means the class distribution is closer to the desired results. Thus, we rank hidden nodes in the ascending order of SNS.

Note that the ranking generated by SNS with binary distribution is similar to the ranking made by classification accuracy. Specifically, if we use a threshold, 0.5, on activation values to separate class 1 from class 0, the classification accuracy for class 1 (CA_1) is

$$\text{CA}_1 = \sum_{r \geq k/2} p(B_r, \mathbf{a}_s) q_r + \sum_{r < k/2} p(B_r, \mathbf{a}_s) (1 - q_r). \quad (14)$$

Similarly, we can construct CA_0 by replacing q_r with $1 - q_r$. Then the best classifying node has the highest classification accuracy. In this paper, our goal is not to obtain the most accurate classification performance, but to understand what the hidden nodes have learned through the unsupervised training process. Moreover, the actual computation of the classification accuracy does not require a histogram. We prefer using cross-entropy because together with the NED values they can reveal more information about the shape of the histograms, which can be used to interpret the learning behaviors in hidden nodes.

5. Experiments

To demonstrate how the proposed node saliency methods evaluate the learning behavior of hidden nodes, we use a simple neural network architecture for a thorough explanation. We select two real data sets for experiments, including images of handwritten digits and breast cancer gene expression. The data set of the handwritten digits is a widely known benchmark that have been used for testing several machine learning methods [20]. In this paper, we are not aiming at a better classification on the digits. Instead, we use this data set for

visualizing the learning tasks made by hidden nodes. In addition, we use the gene expression data sets to make use of their unbalanced clinical features. We train two autoencoder models, each for a selected data set. The optimal decision variables are then employed to create the latent representations. Finally, we address the use of our proposed methods on the latent representations. The description of the data sets and the experimental settings is as follows.

5.1. Data sets

1. The MNIST data set. The Modified National Institute of Standards and Technology (MNIST) data set [20] is a large collection of handwritten digits, constructed from a variety of scanned documents, normalized in size and centered. Each image is a 28 by 28 pixel square (784 pixels total). There are ten digits (0 to 9) in MNIST, which are roughly evenly distributed in the data set. We flatten each image into a 784 dimensional vector. Each element in a vector is a value between zero and one, describing the color intensity of a pixel. Since our supervised ranking methods are designed for classifying data points into two classes, we choose four pairs of digits, including $\{0, 1\}$, $\{2, 7\}$, $\{8, 9\}$ and $\{4, 9\}$, for the experiments. It is known that digits $\{4, 9\}$ are a frequent confusing pair to classify, and that digit 4 and digit 8 are among the most difficult digits to classify [21]. We use the standard partition of MNIST [20] that contains 55,000 data points in the training set, 5,000 in the validation and 10,000 in the test set. The number of samples from each class is listed in Table 1.
2. Breast cancer gene expression data sets. We use the Molecular Taxonomy of Breast Cancer International Consortium (METABRIC) [22] cohort as a training set and the cohort from The Cancer Genome Atlas (TCGA) [23] as an independent evaluation (test) set. The METABRIC contains tumor and normal cells that are described using 2520 gene expression variables that are numerical. The tumor cells are also labeled by the patients' estrogen receptor (ER) status, which can be positive or negative. The METABRIC contains 2136 data points. The validation set for METABRIC is a random 10% partition of the full data, making 214 data points for validation and 1922 data points for training. Table 2 lists the number of data points from each of the class labels in METABRIC and TCGA data sets. Note that the labels in both data sets are highly unbalanced. For example, 93% of data points in METABRIC are from tumor cells while only 7% are from normal cells.

5.2. Autoencoder implementation

While there are several variants of autoencoders [1], the proposed node saliency methods do not depend on the type of autoencoders. Our goal is to explain the learning tasks made by hidden nodes. To give a clear interpretation, we use a basic autoencoder, which has one hidden layer with m hidden nodes. After obtaining the optimal latent representations from one layer, we are able to show that the proposed methods can be used to rank the hidden nodes and

Table 1: Number of data points in pairs of digits from MNIST data set. The data set is divided into a training set and a test set.

Class label	Training set	Test set
0	5,923 (47%)	980 (46%)
1	6,742 (53%)	1,135 (54%)
Total	12,665	2,115
2	5,958 (49%)	1,032 (50%)
7	6,265 (51%)	1,028 (50%)
Total	12,223	2,060
8	5,851 (50%)	974 (49%)
9	5,949 (50%)	1,009 (51%)
Total	11,800	1,983
4	5,842 (50%)	982 (49%)
9	5,949 (50%)	1,009 (51%)
Total	11,791	1,991

Table 2: Number of data points of each ER status and each sample type in METABRIC and TCGA data sets.

Class label	METABRIC	TCGA
ER+	1518 (76%)	396 (77%)
ER-	474 (24%)	117 (23%)
Total	1992	513
Tumor	1992 (93%)	525 (96%)
Normal	144 (7%)	22 (4%)
Total	2136	547

identify significant features from the input layer. Extension to understanding multiple layers is possible and is left for future work. Our autoencoder model is trained with the following architecture: d input variables encoded to m features and reconstructed back to the original d dimension. Specifically, $d = 2520$ and $m = 100$ for METABRIC gene expression data sets, while $d = 784$ and $m = 256$ for MNIST handwritten digits. We trained the autoencoders with the sigmoid activation function and the Adam optimizer [24] using TensorFlow (version 1.0.1) in Python.

5.3. Training autoencoders

Our proposed node saliency methods depend on a well trained autoencoder. To determine an appropriate parameter setting for the data sets described in Section 5.1, we perform a full factorial design over all combinations of selected parameters for each data set. The values of the parameters are determined from a wide range of random selections and then narrowed down to those that give better performances. We split each data set into a training set and a validation set. We do not learn anything from the validation set. Instead, we use it to evaluate the model during the training process, making sure that what we have learned can actually generalize. We apply two measurements, the mean loss and the Pearson correlation coefficient, for both training and validation sets at each epoch. A good learning performance has consistently small loss and high Pearson correlation (whose maximum is one) on both sets.

The training results show that for MNIST data set, using mean squared error as the loss function in autoencoder gives higher Pearson correlations than

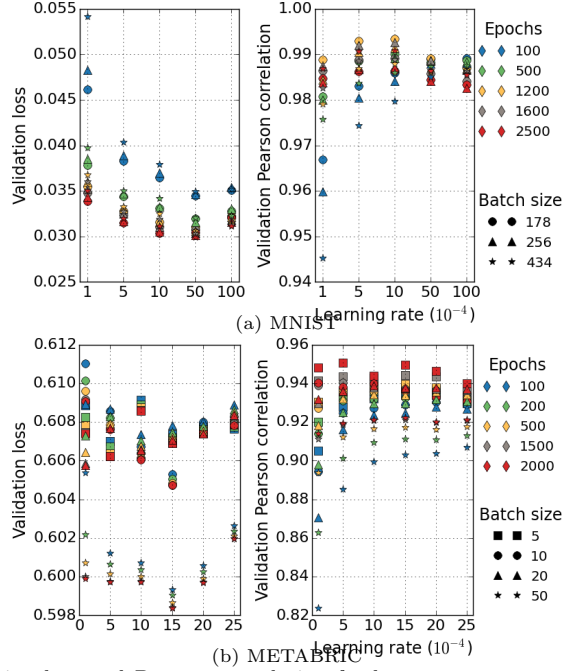


Figure 1: Validation loss and Pearson correlation for key parameters used in training. (a) Best parameter setting for MNIST data set is: batch size 178, learning rate 0.001 and 1200 epochs. (b) Best parameter setting for METABRIC data set is: batch size 5, learning rate 0.0005 and 2000 epochs.

using cross-entropy loss; while for METABRIC, using cross-entropy loss performs better. In general, training results are quite consistent with validation for many parameter combinations, but become worse for larger batches. Training using lower learning rates takes more epochs to converge. Figure 1(a) and (b) summarize the validation loss as well as the Pearson correlation for all parameters used in training the autoencoders on MNIST and METABRIC data sets, respectively. The best parameter combination for MNIST data set is batch size 178, learning rate 0.001 and 1200 epochs, while for METABRIC data set is batch size 5, learning rate 0.0005 and 2000 epochs.

5.4. Experimental settings

After training the autoencoders, we obtain optimal \mathbf{W}^* and \mathbf{b}^* for each of the two data sets, MNIST and METABRIC, based on their best parameter combinations. With the \mathbf{W}^* and \mathbf{b}^* , we can create a latent representation for any data point of the same input variables. Given two class labels, we collect data points of the two labels and construct their latent representations \mathbf{A} . The latent representations for the data points can be observed in m hidden nodes. That is $\mathbf{A} = [\mathbf{a}_s]_{s=1, \dots, m}$. For a hidden node s , we can generate a histogram of the activation values \mathbf{a}_s for the collected data points and count the number of data points in all bins with and without class labels. Then, we can compute

NED on both classes combined, NED_0 and NED_1 for individual classes, and SNS, using (6), (7) and (13), respectively.

To discover whether the autoencoder has learned any properties in the data without knowing the class labels, we rank all hidden nodes according to SNS values. Two rankings are generated, one by SNS with the increasing probability distribution and one by SNS with the binary distribution. We conduct this process for all paired class labels listed in Table 1 and Table 2. Then, a comparison between the increasing probability distribution and the binary distribution is performed.

Furthermore, we evaluate the training results by applying the optimal settings on the designated test sets that are different from the training sets. The latent representations of the test sets at the best ranked nodes are generated using the optimal \mathbf{W}^* and \mathbf{b}^* . We evaluate the performance of the top ranked nodes based on how well they perform on classifying their latent representations of the test set.

Note that we do not use any class labels when training autoencoders. The class labels are used only when generating histograms and computing the supervised node saliency.

6. Experimental results and discussion

In this section, we present the results of our designed experiments that apply the node saliency methods on autoencoder hidden nodes with real data sets. We discuss the insights obtained from the histograms of top ranked nodes as well as the use of node saliency values.

6.1. Ranking the hidden nodes

Given two class labels, the 256 hidden nodes of autoencoders trained on the MNIST training set are ranked by the supervised node saliency (SNS) defined in (13). Figure 2 and Figure 3 display histograms of the activation values from the top two nodes that have the lowest SNS with the increasing probability distribution and the lowest SNS with the binary distribution, respectively. The two figures indicate that using SNS with the binary distribution successfully finds the best classifying nodes for labels $\{0, 1\}$, $\{2, 7\}$ and $\{8, 9\}$, while using SNS with the increasing probability distribution fails at ranking classifying nodes. For separating digit 0 from digit 1, histograms in Figure 2 indicate that the ranked second best node (node 96) distinguishes the two digits better than the ranked top one node (node 201) with increasing probability distribution. Differently, histograms in Figure 3 show that using the binary distribution finds a better classifying node (node 127) and ranks it the top one. Both distributions find node 96 the second best classifying node. For all the three pairs of digits, SNS with the binary distribution is successful in ranking the top one nodes that apparently perform better than the second best nodes.

The results indicate that for classifying handwritten digits using the trained autoencoder, ranking hidden nodes using SNS with the binary distribution is

better than using SNS with the increasing probability distribution. The increasing probability distribution takes mid-point values of the bins for its class distribution. In a histogram of ten bins, the mid-point value of the tenth bin is 0.95, indicating that the reference probability using the increasing probability distribution at the tenth bin is $p_{10} = 95$ percent. In some cases, this setting may prefer mixed classes in the tenth bin more than a single class. On the contrary, SNS with the binary distribution will always prefer 100 percent of class 1 for half of the bins closer to the activation value at one. The results also verify that ranking using SNS with the binary distribution is similar to the ranking using classification accuracy with a threshold 0.5.

In section 4.2 we identified the property that a good classifying node tends to satisfy both $NED < NED_0$ and $NED < NED_1$. Figure 4 and Figure 5 show the NED values sorted by SNS with the increasing probability distribution and with the binary distribution, respectively. Top nodes sorted by SNS with the increasing probability distribution do not have such a property, except for the top nodes for the pair $\{0,1\}$ that are good classifying nodes. On the contrary, most top nodes sorted by SNS with the binary distribution have NED smaller than both NED_0 and NED_1 , meaning that they are good classifying nodes. Especially, the result is consistent with the histograms of the top two nodes shown in Figure 3. Moreover, the rest of the nodes do not have such a property and their NED values are closely aligned together. When the distributions of each single class are almost the same as the whole data distribution, it means that there exists no obvious classification on that latent representations. Therefore, SNS with the binary distribution successfully ranks the classifying nodes and evaluates the trained autoencoder for its ability to classify the three pairs of digits.

The property of NED values for a good classifying node can also be observed on the forth best classifying node ranked by SNS with the increasing probability distribution for MNIST digits $\{2,7\}$. Table 3 lists the NED values of the top seven nodes from the second graph in Figure 4. Among the top nodes, only the forth node (node 122) has the property that both $NED < NED_0$ and $NED < NED_1$. Indeed, with this property being satisfied, node 122 provides good classification performance that is ranked as the second best by SNS with the binary distribution (see Figure 3(b)).

Table 3: Top NED values sorted by SNS with the *increasing probability distribution* as the fixed reference distribution using the pair of digits $\{2,7\}$ in MNIST training set. The forth best node has the property that both $NED < NED_0$ and $NED < NED_1$.

Rank	Node#	SNS _i	NED	NED ₀	NED ₁
1	170	-1.1332	0.6451	0.5666	0.9885
2	150	-0.9368	0.9967	1.0000	0.9938
3	236	-0.9291	0.9771	0.9814	0.9665
4	122	-0.9268	0.5052	0.9242	0.7246
5	78	-0.9219	0.9596	0.9415	0.9704
6	68	-0.9069	0.9529	0.9632	0.9224
7	241	-0.8957	0.9451	0.9375	0.9281

Moreover, the SNS values allow us to compare different classification tasks.

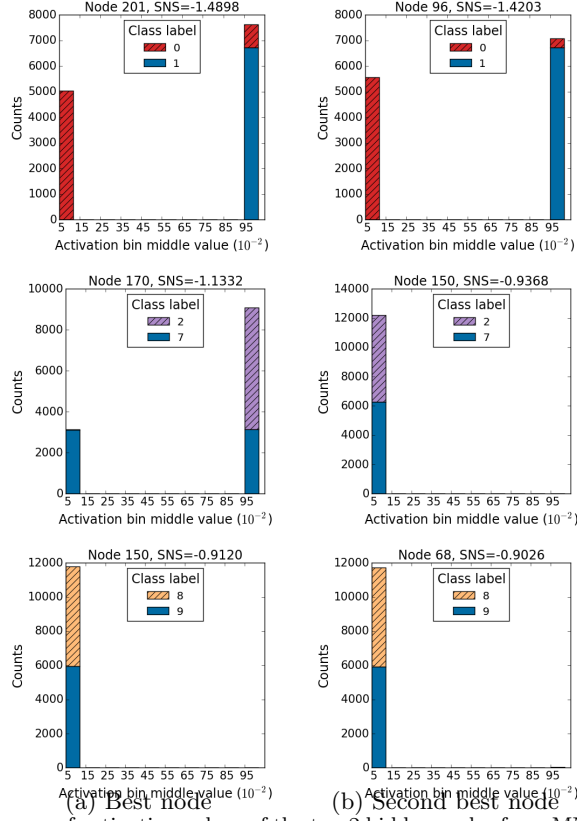


Figure 2: Histograms of activation values of the top 2 hidden nodes from MNIST training set. Three pairs of labels are considered: $\{0,1\}$, $\{2,7\}$, and $\{8,9\}$. The hidden nodes are ranked by SNS with the *increasing probability distribution*. (a) Best node (b) Second best node.

Since we use a simple network design for the autoencoder, the network may not be sufficient enough to capture features that can help in distinguish challenging learning tasks. As shown in Figure 6, the top two hidden nodes (nodes 234 and 89) ranked by SNS with the binary distribution hardly separates the digits $\{4,9\}$, which is known as a difficult task. The node 234 has SNS equal to 0.4357, which is larger than the SNS values of other best nodes with the same fixed reference distribution. For example, as shown in Figure 3, the SNS values of the top nodes that perform better in classification are smaller, which are 0.0404 for node 127, 0.0943 for node 195 and 0.1373 for node 145.

The four pairs of digits from the MNIST test sets are transformed into latent representations and their distributions are displayed in histograms at the best classifying nodes as shown in Figure 7. The histograms illustrate that the best classifying nodes give consistent classification performance on the test sets. The three nodes (i.e. nodes 127, 195 and 145) are still good classifiers. On the other hand, node 234 for the pair of digits $\{4,9\}$ continues to have many misclassified digits.

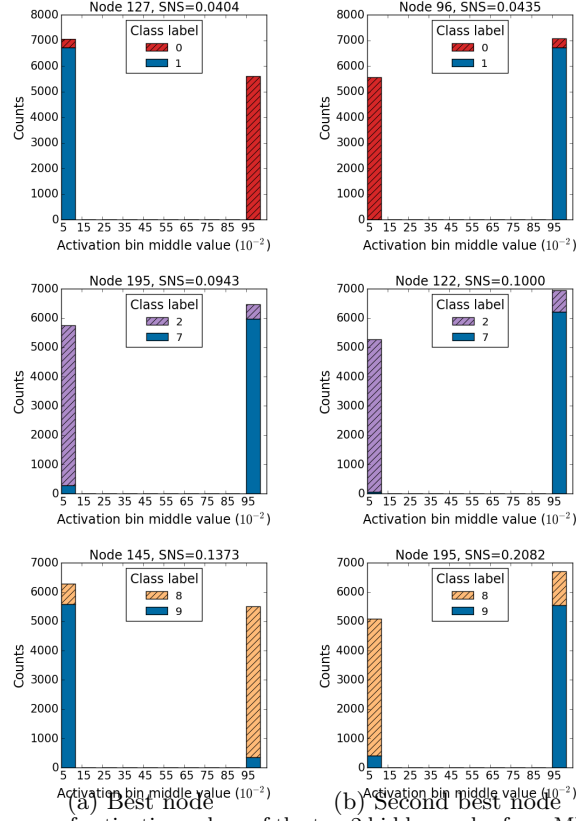


Figure 3: Histograms of activation values of the top 2 hidden nodes from MNIST training set. Three pairs of labels are considered: $\{0,1\}$, $\{2,7\}$, and $\{8,9\}$. The hidden nodes are ranked by SNS with the *binary distribution*. (a) Best node (d) Second best node.

6.2. Misclassified data points

When two classes are well but not perfectly separated in a best classifying node, its histogram of activation values also presents a group of misclassified data points, which exhibits properties similar to the estimated class. Those similar properties that are hard to distinguish could be a common challenge that supervised learning methods need to overcome. We list a few misclassified digits from MNIST data set in Figure 8. By visualizing the patterns in the misclassified digits, a large proportion of the digits could be considered as recognizable by humans without any ambiguity. There is a small group of digits that are either too distorted or ambiguous. If a new handwritten digit has similar characteristics to those misclassified digits, we know that with a high probability it will also be misclassified. Hence, to improve a learning process we need to specifically examine the properties of those misclassified data points.

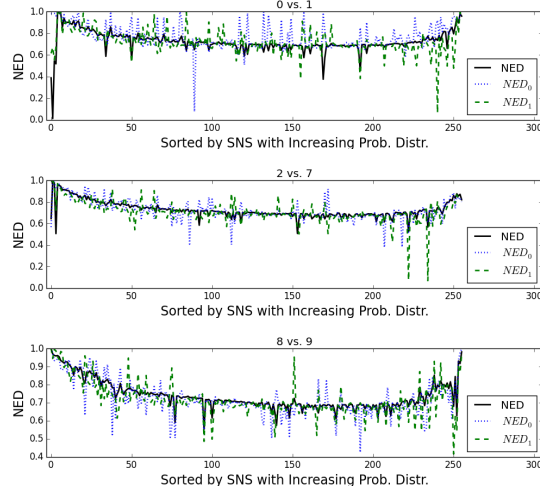


Figure 4: NED values of all hidden nodes, sorted by SNS with the *increasing probability distribution* on MNIST training data for each of the three pairs of labels: $\{0,1\}$, $\{2,7\}$, and $\{8,9\}$.

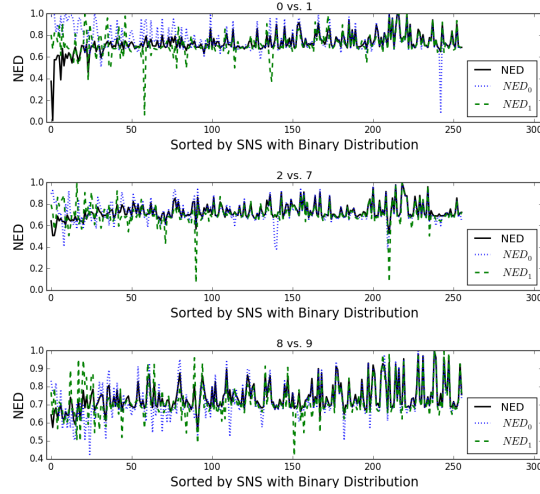


Figure 5: NED values of all hidden nodes, sorted by SNS with the *binary distribution* on MNIST training data for each of the three pairs of labels: $\{0,1\}$, $\{2,7\}$, and $\{8,9\}$.

6.3. Weights of the best classifying nodes

Equation (4) indicates that the latent representations at node s is constructed by putting the weights on the original features of the data \mathbf{X} with the vector \mathbf{w}_s and adding a bias term ($b_s \cdot \mathbf{1}$) as the input of the sigmoid function; where \mathbf{w}_s is the s -th row of the weight matrix \mathbf{W} , and b_s is the s -th element of the bias \mathbf{b} . Therefore, once we identified the best classifying node

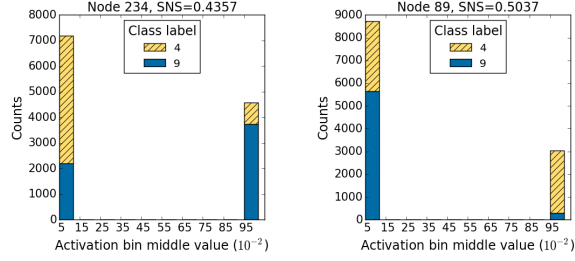


Figure 6: Histograms of the top two classifying nodes from MNIST training set using digits {4,9}, known to be among the most frequent confusing pairs.

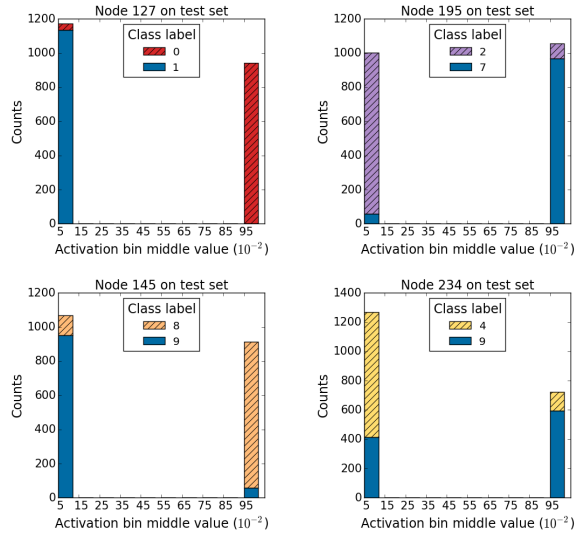


Figure 7: Histograms of the MNIST *test* sets using the four best nodes, each for classifying one of the four pairs of the digits: node 127 for {0,1}, node 195 for {2,7}, node 145 for {8,9} and node 234 for {4,9}.

s , we are able to examine the original features using \mathbf{w}_s^* from the optimal \mathbf{W}^* and learn what features contribute to the classifying task.

The original features of the data points in MNIST data set are the 28 by 28 pixels. Thus, we can visualize a weight vector in a 28 by 28 matrix. The weight vectors for the best classifying nodes are shown in Figure 9. In general most elements in the weight matrix are zero. Larger quantities of positive and negative weights are at the borders of the images.

Specifically, node 127 contains a region in the center where there are weight values that are slightly less than zero. These region does not appear in the other three nodes, indicating critical features for distinguishing digit 0 and digit 1. Similarly, there is a region of pixels at the bottom left of the weight image for node 195, specifying important features for separating digit 2 from digit 7. Those weight values are also less than zero. From the histogram of node 145, we know that classifying digits {8,9} is more difficult than the previous two

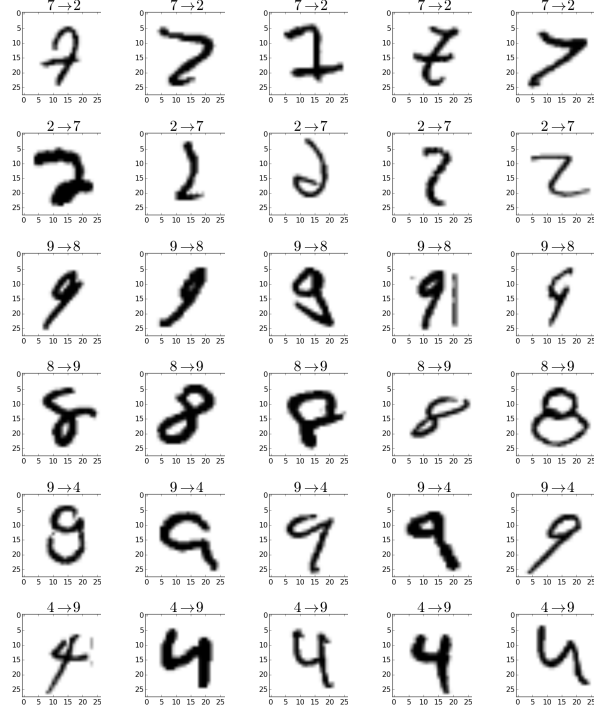


Figure 8: Misclassified digits. The label above the image indicates: True digits \rightarrow Estimated digits.

pairs. The weight image for node 145 shows little regions that clearly suggest important features. Still, there exist regions in the middle that could play a role in classifying digit 8 and digit 9. Finally, node 234 for the pair $\{4,9\}$, one of the most confusing pairs, also has a region of pixels at the top middle that exhibits significant features. The weight vectors from top classifying nodes reveal explanatory input features that contribute to the learning tasks.

6.4. Unbalanced data

The METABRIC data set contains two unbalanced clinical features: sample type and ER status. After training an autoencoder on METABRIC data set with 100 hidden nodes, we obtain optimal decision variables, including the weight matrix \mathbf{W}^* and the bias \mathbf{b}^* . They are used to produce latent representations of the unbalanced classes. We compute the supervised node saliency (SNS) values on the latent representations and use them to rank the 100 hidden nodes.

Figure 12(a) and Figure 12(b) display the NED values sorted by SNS with the increasing probability distribution and with the binary distribution, respectively. Both fixed reference distributions give the same best nodes for the two classification tasks. They are node 55 for tumor vs. normal cells and node 61

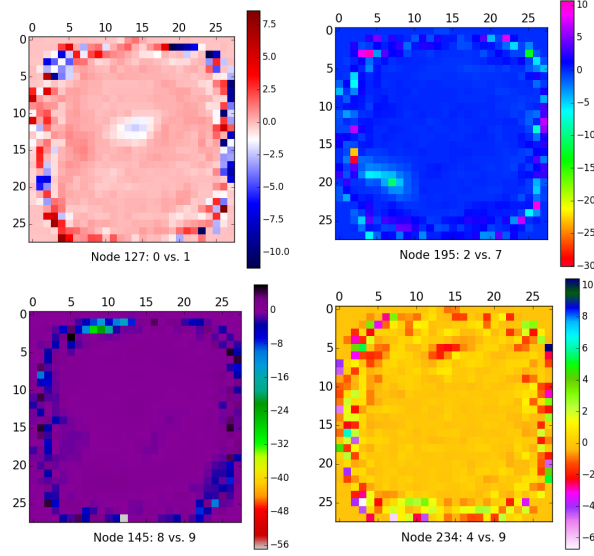


Figure 9: Visualizing weight vectors for the best classifying nodes: node 127 for $\{0,1\}$, node 195 for $\{2,7\}$, node 145 for $\{8,9\}$ and node 234 for $\{4,9\}$, which are ranked by SNS with the binary distribution. The weights are projected to a 28 by 28 matrix, representing weights on pixels.

for ER+ vs. ER-. Both nodes also satisfy the property of a good classifying node where both $NED < NED_0$ and $NED < NED_1$. We observe that except the top few nodes, the NED curves tend to align with NED_1 curves, which is computed based on the major class. This is expected on data sets with unbalanced labels where the distribution of the whole data set turns out to represent the distribution of the major class. The NED values show that the autoencoder is able to learn properties of unbalanced data, and our proposed SNS methods provide useful rankings for finding relevant latent representations.

Figure 10(a) shows the histograms of the latent representations from the METABRIC data set at their best classifying nodes. Node 55 successfully distinguishes the highly unbalanced two classes, including the minority from the normal cells and the majority from the tumor cells, with only a few tumor cells misclassified. Similarly, node 61 classifies ER+ and ER- with a slight error. Using the same optimal weight matrix \mathbf{W}^* and the bias \mathbf{b}^* from the autoencoder trained on METABRIC data set, we construct the latent representations of the TCGA data set, which is from a different data source and is designated for evaluation. The histograms of the latent representations of the TCGA data set at the two best classifying nodes are shown in Figure 10(b). Node 55 separates tumor cells from normal cells almost perfectly. Although having more misclassified data points with ER- in the TCGA data set, node 61 classifies most of the ER+ and ER- data points. The evaluation results verified that the trained autoencoder is able to handle unbalanced breast cancer gene expression data sets.

We include the histograms of the worst classifying nodes from the METABRIC data set in Figure 11. They illustrate that there exist no classification on the two class labels. Activation values occupy all of the bins. Hence, the worst nodes have lower NED values as shown in the NED curves in Figure 12.

6.5. Redundant nodes

The number of hidden nodes is a user-defined number for a neural network architecture. Our proposed NED curves can help identify the redundant nodes that are not useful for learning tasks. When NED is close to one, it means that near constant activation values occupy only one bin. The hidden node that projects data to near constant values loses information and thus is less desirable to keep.

The NED curves shown in Figure 4 and Figure 5 also contain nodes with high NED values without the property for a good classifying node. In Figure 2 two of the highly ranked nodes (node 150 and node 68) that failed at classifying the given labels also have their NED values close to one. Taking node 150 and node 68 for example, their NED, NED_0 and NED_1 range from 0.94 to one, indicating near constant activation values, as shown in the histograms. Their activation values are also close to zero. Therefore, they are redundant nodes among the 256 hidden nodes used for training an autoencoder on the MNIST data set.

Moreover, we use 100 hidden nodes for the METABRIC data set. The NED curves shown in Figure 12 contain only one hidden node that has all three high NED values, which is node 93, the third best node for classifying sample types. Specifically, its NED, NED_0 and NED_1 equal to 0.95, 1 and 0.95, respectively. This indicate that using 100 hidden nodes is sufficient for the autoencoder to work on the METABRIC data set.

7. Conclusion

Autoencoders are trained without using class labels to learn properties in the data. There is a need to develop methods that can indicate which hidden nodes of an autoencoder are able to handle a given learning task. We propose node saliency methods in order to explain what the trained autoencoders have learned.

We have presented supervised node saliency (SNS), a new evaluation approach for ranking hidden nodes based on their relevance to given learning tasks. The SNS is derived from cross-entropy, which we use to compare the class distribution of activation values against a fixed reference distribution. We consider two fixed reference distributions: the increasing probability distribution and the binary distribution. We apply our methods on two real data sets, MNIST handwritten digits and breast cancer gene expression data sets. Pairs of labels in the data sets are collected for classification tasks. Our experimental results indicate that SNS with the binary distribution provides useful rankings on the hidden nodes based on their classification performance. The class distribution

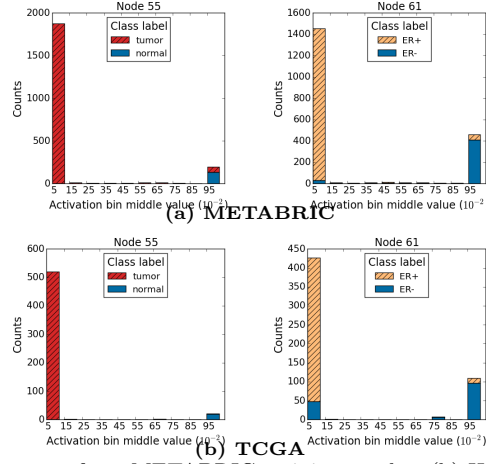


Figure 10: (a) Histograms from METABRIC training results. (b) Histograms from TCGA evaluation results. The best nodes ranked by SNS on the METABRIC data sets for each pair of the classes are: node 55 for classifying tumor and normal cells, and node 61 for distinguishing ER+ and ER-. Both fixed reference distributions, including the increasing probability distribution and the binary distribution, used in SNS give the same top nodes.

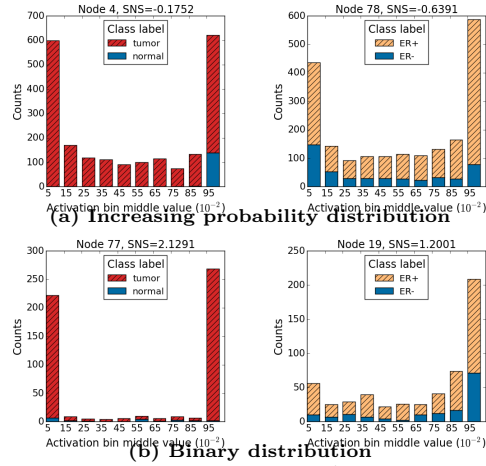


Figure 11: Histograms of the worst nodes from METABRIC training results. (a) The worst nodes ranked by SNS with the increasing probability distribution (b) The worst nodes ranked by SNS with the binary distribution.

in the breast cancer gene expression data is highly unbalanced. We demonstrate that SNS is able to identify the best classifying node even for unbalanced data.

We discover a condition for identifying a good classifying node using normalized entropy difference (NED) and its modified form NED_0 for class 0 and NED_1 for class 1. Since the NED values are between zero and one, we are able to compare histograms of latent representations at different nodes in terms of their “interestingness”. We show that the node saliency methods can be used

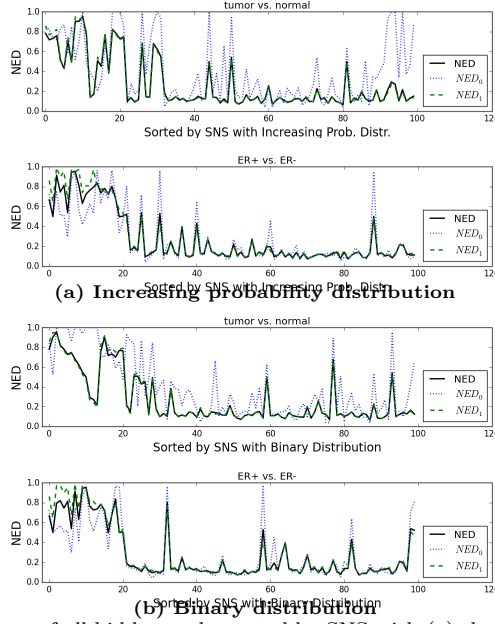


Figure 12: NED values of all hidden node, sorted by SNS with (a) the increasing probability distribution (b) the binary distribution on METABRIC data, each with two pairs of labels: tumor v.s. normal, and ER+ v.s.ER-.

to identify which hidden node is able to classify the data. The corresponding weight vector of the best classifying node can be used to explain which of the input features contribute to the learning task. We visualize the contributing features with the MNIST data set. Future work would extend these methods from the current single layer architecture to a multi-layer neural network.

Acknowledgments

LLNL-JRNL-741590. This work has been supported in part by the Joint Design of Advanced Computing Solutions for Cancer (JDACS4C) program established by the U.S. Department of Energy (DOE) and the National Cancer Institute (NCI) of the National Institutes of Health. This work was performed under the auspices of the U.S. Department of Energy by Lawrence Livermore National Laboratory under Contract DE-AC52-07NA27344.

References

- [1] G. E. Hinton, R. S. Zemel, Autoencoders, minimum description length and helmholtz free energy, in: J. D. Cowan, G. Tesauro, J. Alspector (Eds.), Advances in Neural Information Processing Systems 6, Morgan-Kaufmann, 1994, pp. 3–10.

- [2] I. Goodfellow, Y. Bengio, A. Courville, Deep Learning, MIT Press, 2016, <http://www.deeplearningbook.org>.
- [3] Development Organization Workgroup ASN-0002, American Type Culture Collection Standards, Cell line misidentification: the beginning of the end, Nature Reviews Cancer 10.
- [4] M. Allen, M. Bjerke, H. Edlund, S. Nelander, B. Westermarck, Origin of the u87mg glioma cell line: Good news and bad news, Science Translational Medicine 8 (354) (2016) 354re3.
- [5] P. Baldi, K. Hornik, Neural networks and principal component analysis: Learning from examples without local minima, Neural Netw. 2 (1) (1989) 53–58.
- [6] J. Tan, M. Ung, C. Cheng, C. S. Greene, Unsupervised feature construction and knowledge extraction from genome-wide assays of breast cancer with denoising autoencoders, Pacific Symposium on Biocomputing 20 (2015) 132–143.
- [7] G. P. Way, C. S. Greene, Extracting a biologically relevant latent space from cancer transcriptomes with variational autoencoders, bioRxiv.
- [8] L. M. Zintgraf, T. S. Cohen, T. Adel, M. Welling, Visualizing deep neural network decisions: Prediction difference analysis, CoRR abs/1702.04595. [arXiv:1702.04595](https://arxiv.org/abs/1702.04595).
- [9] A. Shrikumar, P. Greenside, A. Kundaje, Learning important features through propagating activation differences, CoRR abs/1704.02685.
- [10] K. Simonyan, A. Vedaldi, A. Zisserman, Deep inside convolutional networks: Visualising image classification models and saliency maps, CoRR abs/1312.6034. [arXiv:1312.6034](https://arxiv.org/abs/1312.6034).
- [11] S. Gilles, Robust Matching and Description of Images, PhD thesis, Oxford University, 1998.
- [12] T. Kadir, M. Brady, Saliency, scale and image description, International Journal of Computer Vision 45 (2) (2001) 83–105.
- [13] C. Kamath, A. Gezahegne, S. D. Newsam, G. M. Roberts, Salient points for tracking moving objects in video, in: Image and Video Communications and Processing, 2005, pp. 442–453.
- [14] S. Byttner, T. Rögnvaldsson, M. Svensson, Consensus self-organized models for fault detection (cosmo), Eng. Appl. Artif. Intell. 24 (5) (2011) 833–839.
- [15] Y. Fan, S. Nowaczyk, T. Rögnvaldsson, E. A. Antonelo, Predicting air compressor failures with echo state networks, in: Third European Conference of the Prognostics and Health Management Society 2016, Vol. 7, 2016, pp. 568–578.

- [16] T. Rögnavaldsson, S. Nowaczyk, S. Byttner, R. Prytz, M. Svensson, Self-monitoring for maintenance of vehicle fleets, *Data mining and knowledge discovery*.
- [17] S.-H. Cha, Comprehensive survey on distance/similarity measures between probability density functions, *International Journal of Mathematical Models and Methods in Applied Sciences* 1 (4) (2007) 300–307.
- [18] O. Pele, Distance functions: Theory, algorithms and applications, Ph.D. thesis, The Hebrew University of Jerusalem (2011).
- [19] G. E. Hinton, Connectionist learning procedures, *Artificial Intelligence* 40 (1) (1989) 185 – 234.
- [20] Y. LeCun, L. Bottou, Y. Bengio, P. Haffner, Gradient-based learning applied to document recognition, *Proceedings of the IEEE* 86 (11) (1998) 2278–2324.
- [21] F. Lauer, C. Y. Suen, G. Bloch, A trainable feature extractor for handwritten digit recognition, *Pattern Recognition* 40 (6) (2007) 1816–1824.
- [22] C. Curtis, S. P. Shah, S.-F. Chin, G. Turashvili, O. M. Rueda, M. J. Dunning, D. Speed, A. G. Lynch, S. Samarajiwa, Y. Yuan, S. Graf, G. Ha, G. Haffari, A. Bashashati, R. Russell, S. McKinney, A. Langerod, A. Green, E. Provenzano, G. Wishart, S. Pinder, P. Watson, F. Markowitz, L. Murphy, I. Ellis, A. Purushotham, A.-L. Borresen-Dale, J. D. Brenton, S. Tavaré, C. Caldas, S. Aparicio, The genomic and transcriptomic architecture of 2000 breast tumours reveals novel subgroups, *Nature* 486 (2012) 346–352.
- [23] The Cancer Genome Atlas Network, Comprehensive molecular portraits of human breast tumours, *Nature* 490 (2012) 61–70.
- [24] D. P. Kingma, J. Ba, Adam: A method for stochastic optimization, CoRR abs/1412.6980.